Vector analysis and control of advanced static VAR compensators

C. Schauder
H. Mehta

Indexing terms: Inverters, Power transmission, Static VAR compensators

Abstract: The advanced static VAR compensator (now widely known as the static condenser or STATCON) uses a high power self-commutating inverter to draw reactive current from a transmission line. Two fundamentally different types of invertor can be used for this purpose, one providing control of output voltage magnitude and phase angle, and the other having only phase angle control. For each of these types, the governing equations are derived, and frequency domain analysis is used to obtain the relevant transfer functions for control system synthesis. Further analysis is provided to determine the response of the STATCON to negative sequence and harmonic voltage components on the transmission line. The results are illustrated with measured waveforms obtained from a scaled analogue model of an 80 MVAR STATCON.

1 Introduction

The advanced static VAR compensator (ASVC) is based on the principle that a self-commutating static inverter can be connected between three-phase AC power lines and an energy-storage device, such as an inductor or capacitor, and controlled to draw mainly reactive current from the lines. This capability is analogous to that of the rotating synchronous condenser and it can be used in a similar way for the dynamic compensation of power transmission systems, providing voltage support, increased transient stability, and improved damping [1, 2]. The ASVC inverter requires gate-controlled power switching devices such as GTO thyristors. GTOs are now available with ratings that are sufficiently high to make transmission line applications feasible. Consequently the ASVC has become an important part of the flexible AC transmission system (FACTS), introduced by Hingorani [3], and presently being promoted by the Electric Power Research Institute (EPRI).

The EPRI has recently commissioned the design and construction of a scaled model of an 80 MVAR ASVC for transmission lines [4]. The model represents an optimum power circuit configuration based on a voltage-sourced inverter, and includes the control system that would be applied to a fullpower installation. The control system has been designed to achieve fast dynamic control of the instantaneous reactive current drawn from the line. This capability ensures that the ASVC will function usefully during transmission line disturbances. The concept of instantaneous reactive current is a new one and will be explained in the following Sections.

In the course of this project, the dynamic behaviour of the ASVC has been studied in depth. This paper presents a simplified mathematical model of the ASVC that has made it possible to derive the transfer functions needed for control system synthesis. The resulting control system designs are briefly outlined and further analysis presented to show the behaviour of the ASVC when the line voltage is unbalanced or distorted. The analysis is based on a vectorial transformation of variables, first described by Park [5] for AC machine analysis, and later, using complex numbers, by Lyon [6] in the theory of instantaneous symmetrical components.

2 Derivation of ASVC mathematical model

2.1 Instantaneous reactive current

The main function of the ASVC is to regulate the transmission line voltage at the point of connection. It achieves this objective by drawing a controlled reactive current from the line. In contrast with a conventional static VAR generator, the ASVC also has the intrinsic ability to exchange real power with the line. As there are no sizeable power sources or sinks associated with the inverter and its DC-side components, the real power must be actively controlled to a value which is zero on average and which departs from zero only to compensate for the losses in the system.

The notion of reactive power is well known in the phasor sense. However, to study and control the dynamics of the ASVC within a subcycle time frame and subject to line distortions, disturbances and unbalance, we need a broader definition of reactive power which is valid on an instantaneous basis.

The instantaneous real power at a point on the line is given by

$$P = v_a i_a + v_b i_b + v_c i_c \quad (1)$$

Paper 9274C (P7), first received 12th December 1991 and in revised form 2nd November 1992

Dr. Schauder is with Westinghouse STC, 601-1A53D, 1310 Baulah Road, Pittsburgh, PA 15235, USA

Dr. Mehta is with the Electric Power Research Institute,

The ASVC scaled model was designed and built at the Westinghouse Science and Technology Center through the combined efforts of several individuals. In particular, the authors would like to acknowledge the important contributions made by Mr. M. Gernhardt and Mr. M. Brennen.

We can define the instantaneous reactive current conceptually as that part of the three-phase current set that could be eliminated at any instant without altering P.

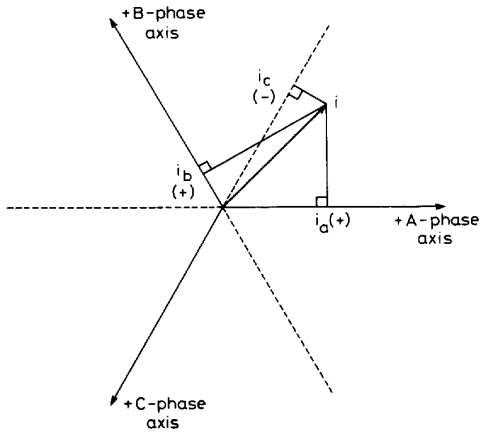

Fig. 1 *Vector representation of instantaneous three-phase variables*

The algebraic definition of instantaneous reactive current is obtained by means of a vectorial interpretation of the instantaneous values of the circuit variables, as explained in the following Section.

2.2 Vector representation of instantaneous three-phase quantities

A set of three instantaneous phase variables that sum to zero can be uniquely represented by a single point in a plane, as illustrated in Fig. 1. By definition, the vector drawn from the origin to this point has a vertical projection onto each of three symmetrically disposed phase axes which corresponds to the instantaneous value of the associated phase variable. This transformation of phase variables to instantaneous vectors can be applied to voltages as well as to currents. As the values of the phase variables change, the associated vector moves around the plane describing various trajectories. The vector contains all the information on the three-phase set, including steady-state unbalance, harmonic waveform distortions, and transient components. Fig. 2 provides a graphical illustration of the vector trajectory that would develop in the case of a three-phase set with severe harmonic distortion. The diagram shows the vector trajectory and relates it back to the actual phase-variable waveforms.

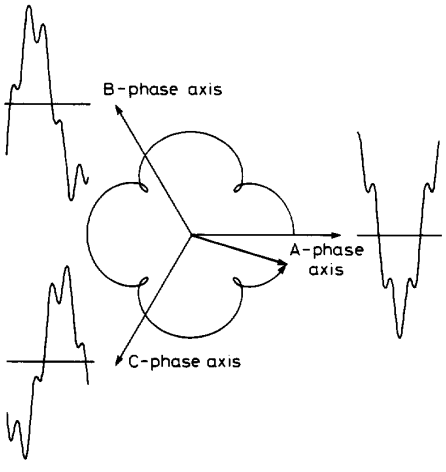

Fig. 2 *Example of vector trajectory: 25% fifth harmonic*

In Fig. 3, the vector representation is extended by introducing an orthogonal co-ordinate system in which each vector is described by means of its ds- and qs-components. The transformation from phase variables to ds and qs co-ordinates is as follows:

$$[c] = \frac{2}{3}\begin{bmatrix} 1 & -\frac{1}{2} & -\frac{1}{2} \\ 0 & \frac{\sqrt{3}}{2} & -\frac{\sqrt{3}}{2} \\ \frac{1}{\sqrt{2}} & \frac{1}{\sqrt{2}} & \frac{1}{\sqrt{2}} \end{bmatrix} \quad [c]^{-1} = \tfrac{3}{2}[c]_t$$

$$\begin{bmatrix} i_{ds} \\ i_{qs} \\ 0 \end{bmatrix} = [c]\begin{bmatrix} i_a \\ i_b \\ i_c \end{bmatrix} \quad \begin{bmatrix} v_{ds} \\ v_{qs} \\ 0 \end{bmatrix} = [c]\begin{bmatrix} v_a \\ v_b \\ v_c \end{bmatrix} \tag{2}$$

Fig. 3 shows how the vector representation leads to the definition of instantaneous reactive current. In the diagram, two vectors are drawn, one to represent the transmission line voltage at the point of connection and the other to describe the current in the ASVC lines.

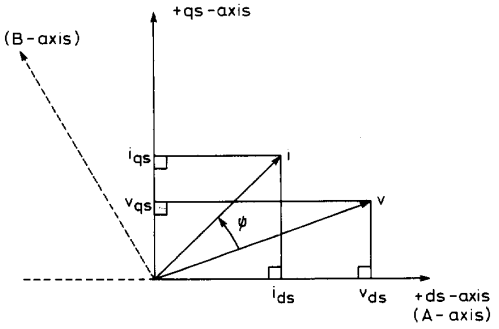

Fig. 3 *Definition of orthogonal co-ordinates*

Using eqns. 2, the instantaneous power given by eqn. 1 can be rewritten in terms of ds and qs quantities as follows:

$$P = \tfrac{3}{2}(v_{ds}i_{ds} + v_{qs}i_{qs}) = \tfrac{3}{2}|v||i|\cos(\phi) \tag{3}$$

where ϕ is the angle between the voltage and the current vectors. Clearly, only that component of the current vector which is in phase with the instantaneous voltage vector contributes to the instantaneous power. The remaining current component could be removed without changing the power, and this component is therefore the instantaneous reactive current. These observations can be extended to the following definition of instantaneous reactive power:

$$Q = \tfrac{3}{2}|v||i|\sin(\phi) = \tfrac{3}{2}(v_{ds}i_{qs} - v_{qs}i_{ds}) \tag{4}$$

where the constant 3/2 is chosen so that the definition coincides with the classical phasor definition under balanced steady-state conditions.

Fig. 4 shows how further manipulation of the vector co-ordinate frame leads to a useful separation of variables for power control purposes. A new co-ordinate system is defined where the d-axis is always coincident with the instantaneous voltage vector and the q-axis is in quadrature with it. The d-axis current component, i_d, accounts for the instantaneous power and the q-axis

current, i_q, is the instantaneous reactive current. The d and q axes are not stationary in the plane. They follow the trajectory of the voltage vector, and the d and q co-ordinates within this synchronously rotating reference

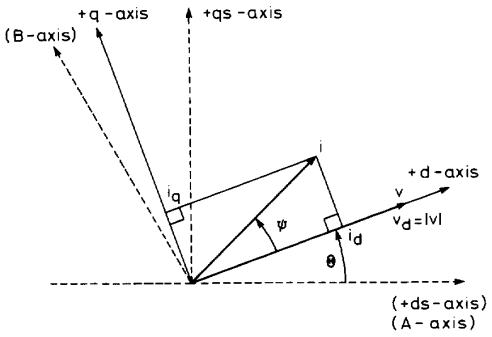

Fig. 4 *Definition of rotating reference frame*

frame are given by the following time-varying transformation:

$$[c_1] = \frac{2}{3}\begin{bmatrix} \cos(\theta) & \cos\left(\theta - \frac{2\pi}{3}\right) & \cos\left(\theta + \frac{2\pi}{3}\right) \\ -\sin(\theta) & -\sin\left(\theta - \frac{2\pi}{3}\right) & -\sin\left(\theta + \frac{2\pi}{3}\right) \\ \frac{1}{\sqrt{2}} & \frac{1}{\sqrt{2}} & \frac{1}{\sqrt{2}} \end{bmatrix}$$

$$[C_1]^{-1} = \tfrac{3}{2}[c_1]_t \quad \theta = \tan^{-1}\left(\frac{v_{qs}}{v_{ds}}\right)$$

$$\begin{bmatrix} i_a \\ i_b \\ i_c \end{bmatrix} [C_1]^{-1} \begin{bmatrix} i_d \\ i_q \\ 0 \end{bmatrix} \quad \begin{bmatrix} v_a \\ v_b \\ v_c \end{bmatrix} = [c_1]^{-1} \begin{bmatrix} |v| \\ 0 \\ 0 \end{bmatrix} \tag{5}$$

and substituting in eqn. 1 we obtain

$$P = \tfrac{3}{2}\{|v| i_d \quad Q = \tfrac{3}{2}|v| i_q \tag{6}$$

Under balanced steady-state conditions, the co-ordinates of the voltage and current vectors in the synchronous reference frame are constant quantities. This feature is useful for analysis and for decoupled control of the two current components.

2.3 Equivalent circuit and equations

Fig. 5 shows a simplified representation of the ASVC, including a DC-side capacitor, an inverter, and series inductance in the three lines connecting to the transmission line. This inductance accounts for the leakage of the actual power transformers. The circuit also includes resistance in shunt with the capacitor to represent the switching losses in the inverter, and resistance in series with the AC lines to represent the inverter and transformer conduction losses. The inverter block in the circuit is treated as an ideal, lossless power transformer.

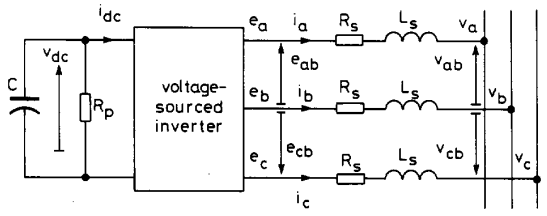

Fig. 5 *Equivalent circuit of ASVC*

In terms of the instantaneous variables shown in Fig. 5, the AC-side circuit equations can be written as follows:

$$p\begin{bmatrix} i'_a \\ i'_b \\ i'_c \end{bmatrix} = \begin{bmatrix} \frac{-R'_s\omega_b}{L'} & 0 & 0 \\ 0 & \frac{-R'_s\omega_b}{L'} & 0 \\ 0 & 0 & \frac{-R'_s\omega_b}{L'} \end{bmatrix} \begin{bmatrix} i'_a \\ i'_b \\ i'_c \end{bmatrix} + \frac{\omega_b}{L'}\begin{bmatrix} (e'_a - v'_a) \\ (e'_b - v'_b) \\ (e'_c - v'_c) \end{bmatrix} \tag{7}$$

where $p = d/dt$, and a per-unit system has been adopted according to the following definitions:

$$L' = \frac{\omega_b L_s}{z_{base}} \quad C' = \frac{1}{\omega_b C z_{base}} \quad R'_s = \frac{R_s}{z_{base}} \quad R'_p = \frac{R_p}{z_{base}}$$

$$i'_x = \frac{i_x}{i_{base}} \quad v'_x = \frac{v_x}{v_{base}} \quad e'_x = \frac{e_x}{v_{base}} \quad z_{base} = \frac{v_{base}}{i_{base}} \tag{8}$$

Using the transformation of variables defined in eqn. 5, eqns. 7 can be transformed to the synchronously rotating reference frame as follows:

$$p\begin{bmatrix} i'_d \\ i'_q \end{bmatrix} = \begin{bmatrix} \frac{-R'_s\omega_b}{L'} & \omega \\ -\omega & \frac{-R'_s\omega_b}{L'} \end{bmatrix} \begin{bmatrix} i'_d \\ i'_q \end{bmatrix} + \frac{\omega_b}{L'}\begin{bmatrix} (e'_d - |v'|) \\ e'_q \end{bmatrix} \tag{9}$$

where $\omega = d\theta/dt$. Fig. 6 illustrates the AC-side circuit vectors in the synchronous frame. When i'_q is positive, the ASVC is drawing inductive VARS from the line, and for negative i'_q it is capacitive.

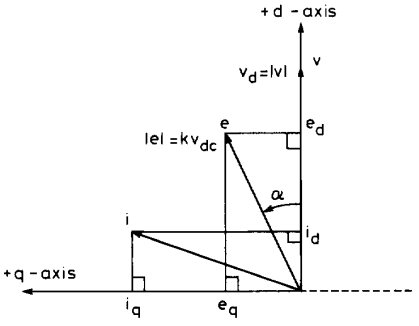

Fig. 6 *ASVC vectors in synchronous frame*

2.4 Types of voltage-sourced inverter

Neglecting the voltage harmonics produced by the inverter, we can write a pair of equations for e'_d and e'_q.

$$e'_d = kv'_{dc} \cos(\alpha) \tag{10}$$

$$e'_q = kv'_{dc} \sin(\alpha) \tag{11}$$

where k is a factor for the inverter which relates the DC-side voltage to the amplitude (peak) of the phase-to-neutral voltage at the inverter AC-side terminals, and α is the angle by which the inverter voltage vector leads the line voltage vector. It is important to distinguish between two basic types of voltage-sourced inverter that can be used in ASVC systems.

Inverter Type I allows the instantaneous values of both α and k to be varied for control purposes. Provided

that v'_{dc} is kept sufficiently high, e'_d and e'_q can be independently controlled. This capability can be achieved by various pulse-width-modulation (PWM) techniques that invariably have a negative impact on the efficiency, harmonic content, or utilisation of the inverter. Type I inverters are presently considered uneconomical for transmission line applications and their control will only be briefly considered here.

Inverter Type II is of primary interest for transmission line ASVCs. In this case, k is a constant factor, and the only available control input is the angle, α, of the inverter voltage vector. This case will be discussed in greater detail.

2.5 Inverter type I control system

Inspection of eqn. 9 leads directly to a rule that will provide decoupled control of i'_d and i'_q. The inverter voltage vector is controlled as follows:

$$e'_d = \frac{L'}{\omega_b}(x_1 - \omega i'_q) + |v'| \tag{12}$$

$$e'_q = \frac{L'}{\omega_b}(x_2 + \omega i'_d) \tag{13}$$

Substitution of eqns. 12 and 13 into eqn. 9 yields

$$p\begin{bmatrix} i'_d \\ i'_q \end{bmatrix} = \begin{bmatrix} \frac{-R'_s\omega_b}{L'} & 0 \\ 0 & \frac{-R'_s\omega_b}{L'} \end{bmatrix}\begin{bmatrix} i'_d \\ i'_q \end{bmatrix} + \begin{bmatrix} x_1 \\ x_2 \end{bmatrix} \tag{14}$$

Eqn. 14 shows that i'_d and i'_q respond to x_1 and x'_2 respectively, through a simple first-order transfer function, with no crosscoupling. The control rule of eqns. 12 and 13 is thus completed by defining the feedback loops and proportional-plus-integral compensation as follows:

$$x_1 = \left(k_a + \frac{k_b}{p}\right)(i'^*_d - i'_d) \tag{15}$$

$$x_2 = \left(k_a + \frac{k_b}{p}\right)(i'^*_q - i'_q) \tag{16}$$

The control is thus actually performed using feedback variables in the synchronous reference frame. The reactive current reference, i'^*_q, is supplied from the ASVC outer-loop voltage control system, and the real power is regulated by varying i'^*_d in response to error in the DC-link voltage via a proportional plus integral compensation. A block diagram of the control scheme is presented in Fig. 7.

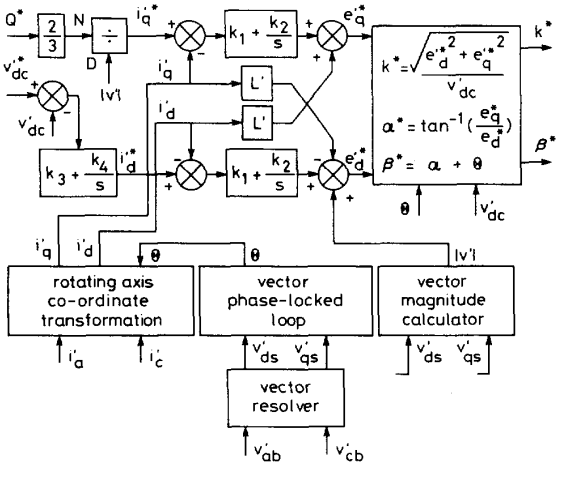

Fig. 7 *Block diagram of inverter Type I control*

2.6 Further model development for inverter type II control

For Type II inverter control it is necessary to include the inverter and DC-side circuit equation in the model. The instantaneous power at the AC- and DC-terminals of the inverter is equal, giving the following power balance equation:

$$v'_{dc} i'_{dc} = \tfrac{3}{2}(e'_d i'_d + e'_q i'_q) \tag{17}$$

and the DC-side circuit equation is

$$pv'_{dc} = -\omega_b C'\left(i'_{dc} + \frac{v'_{dc}}{R'_p}\right) \tag{18}$$

Combining eqns. 9, 10, 11, 17 and 18, we obtain the following state equations for the ASVC:

$$p\begin{bmatrix} i'_d \\ i'_q \\ v'_{dc} \end{bmatrix} = [A]\begin{bmatrix} i'_d \\ i'_q \\ v'_{dc} \end{bmatrix} - \begin{bmatrix} \frac{\omega_b}{L'}|v'| \\ 0 \\ 0 \end{bmatrix}$$

$$[A] = \begin{bmatrix} \frac{-R'_s\omega_b}{L'} & \omega & \frac{k\omega_b}{L'}\cos(\alpha) \\ -\omega & \frac{-R'_s\omega_b}{L'} & \frac{k\omega_b}{L'}\sin(\alpha) \\ \frac{-3}{2}kC'\omega_b\cos(\alpha) & \frac{-3}{2}kC'\omega_b\sin(\alpha) & \frac{-\omega_b C'}{R'_p} \end{bmatrix} \tag{19}$$

Steady-state solutions for eqn. 19 using typical system parameters are plotted in Fig. 8 as a function of α_0 (subscript 0 denotes steady-state values). Note that i'_{q0} varies almost linearly with respect to α_0, and the range of α_0 for one per-unit swing in i'_{q0} is very small. Neglecting losses (i.e. $R'_s = 0$, $R'_p = \infty$), the steady-state solutions

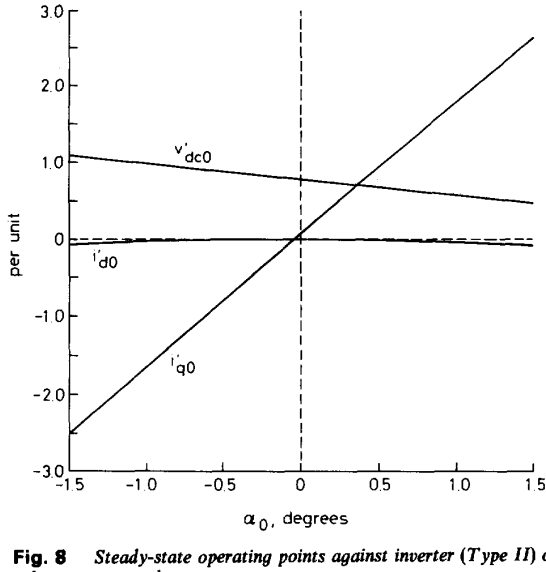

Fig. 8 *Steady-state operating points against inverter (Type II) output voltage vector angle*

$L' = 0.15$, $C' = 0.88$, $k = 4/\pi$, $R'_s = 0.01$, $R'_p = 100/k$, $v'_0 = 1.0$, $\omega_0 = 377$, $\omega_b = 377$

would be is follows:

$$\omega = \omega_b \quad i'_q = i'_{q0} \quad |v'| = v'_0$$

$$\alpha_0 = 0 \quad i'_{d0} = 0 v'_{dc0} = \frac{1}{k}[v'_0 - i'_{q0} L'] \tag{20}$$

2.7 Linearisation of ASVC equations for small perturbations

The ASVC state eqns. 19 are nonlinear if α is regarded as an input variable. We can, however, find useful solutions for small deviations about a chosen steady-state equilibrium point. The linearisation process yields the following perturbation equations:

$$p\begin{bmatrix}\Delta i'_d\\ \Delta i'_q\\ \Delta v'_{dc}\end{bmatrix} = [A_\Delta]\begin{bmatrix}\Delta i'_d\\ \Delta i'_q\\ \Delta v'_{dc}\end{bmatrix} + [B_\Delta]\begin{bmatrix}\Delta v'\\ \Delta\alpha\end{bmatrix}$$

$$[A_\Delta] = \begin{bmatrix} \frac{-R'_s\omega_b}{L'} & \omega_b & \frac{k\omega_b}{L'}\cos(\alpha_0) \\ -\omega_b & \frac{-R'_s\omega_b}{L'} & \frac{k\omega_b}{L'}\sin(\alpha_0) \\ \frac{-3}{2}kC'\omega_b\cos(\alpha_0) & \frac{-3}{2}kC'\omega_b\sin(\alpha_0) & \frac{-\omega_b C'}{R'_p} \end{bmatrix}$$

$$[B_\Delta] = \begin{bmatrix} \frac{-\omega_b}{L'} & \frac{-k\omega_b v'_{dc0}}{L'}\sin(\alpha_0) \\ 0 & \frac{k\omega_b v'_{dc0}}{L'}\cos(\alpha_0) \\ 0 & \frac{3}{2}kC'\omega_b(i'_{d0}\sin(\alpha_0) - i'_{q0}\cos(\alpha_0)) \end{bmatrix} \tag{21}$$

Standard frequency domain analysis can be used to obtain transfer functions from eqns. 21. Numerical methods have been used to obtain specific results, but it is useful to first consider some general results, neglecting the system power losses (i.e. $R'_s = 0$, $R'_p = \infty$). For this case, the block diagram of Fig. 9 shows how the control

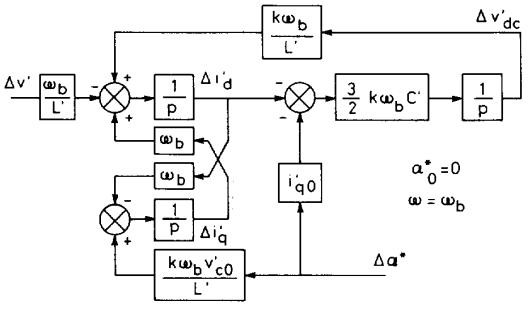

Fig. 9 *Small-signal block diagram showing dynamic behaviour of ASVC system with Type II inverter*

input, $\Delta\alpha$, influences the system states. The corresponding transfer function relating $\Delta i'_q$ and $\Delta\alpha$ is as follows:

$$\frac{\Delta I'_q(s)}{\Delta\alpha(s)} = \frac{L''[s^2 + L'C'']v'_{dc0} + [L''C''\omega_b]i'_{q0}}{s[s^2 + \omega_b^2 + L'C'']} \tag{22}$$

where

$$L' = \frac{k\omega_b}{L} \quad C'' = \frac{3k\omega_b C'}{2}$$

The undamped poles of the system are thus at

$$s = 0 \quad \text{and} \quad s = \pm j\omega_b\sqrt{\left(1 + \frac{3k^2C'}{2L'}\right)} \tag{23}$$

The transfer function, eqn. 22, also has a pair of complex zeroes on the imaginary axis. These move along the imaginary axis as a function of i'_{q0}, occuring at lower frequency than the poles only when

$$i'_{q0} < \frac{2v'_{dc0}}{3kC'} = i'_{q0X} \tag{24}$$

A numerical computation of $\Delta I'_q(s)/\Delta\alpha(s)$ from eqn. 21, including the losses, has been done for two operating points to illustrate the movement of the complex zeroes. Fig. 10A presents the result for each case in a plot of log gain and phase against frequency.

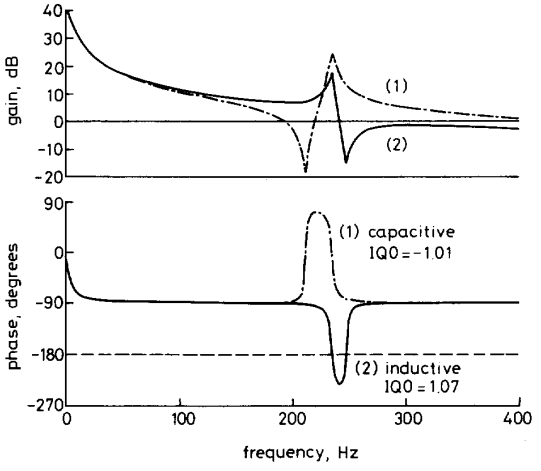

Fig. 10A *Transfer function $\Delta I'q(s)/\Delta\alpha(s)/\Delta\alpha(s)$*
$k = 4/\pi$, $L = 0.15$, $C = 0.88$, $R_s = 0.01$, $R_p = 100.0/k$

Case 1: Full capacitive load

$$i'_{q0} = -1.01 \text{ p.u.} \quad \alpha_0 = -0.011 \text{ rad } (0.63°)$$

$$\frac{\Delta I'_q(s)}{\Delta\alpha(s)} = \frac{2893(s + 8.7 + j1330)(s + 8.7 - j1330)}{(s + 23.8)(s + 15.4 + j1476)(s + 15.4 - j1476)}$$

Case 2: Full inductive load

$$i'_{q0} = 1.07 \text{ p.u.} \quad \alpha_0 = 0.01 \text{ rad } (0.57°)$$

$$\frac{\Delta I'_q(s)}{\Delta\alpha(s)} = \frac{2111(s + 11.4 + j1557)(s + 11.4 - j1557)}{(s + 23.8)(s + 15.4 + j1476)(s + 15.4 - j1476)}$$

While Case 1 is amenable to feedback control, Case 2 clearly has little phase margin near the system resonant frequency. The latter situation is typical for the condition $i'_{q0} > i'_{q0X} = 0.44$ p.u. in this example.) A controller has been designed to overcome this problem by using nonlinear state-variable feedback to improve the phase margin when $i'_{q0} > i'_{q0X}$. The nonlinear feedback function, Δ'_q, has the following form:

$$\Delta q' = \Delta i'_q - g[i'_{q0} - i'_{q0X}]\,\Delta v'_{dc} \tag{25}$$

where g is a gain factor to be set by design. Fig. 10B shows the transfer function, $\Delta Q'(s)/\Delta\alpha(s)$, for the same operating points as Fig. 10A, with $g = 2.0$. The improved phase margin in Case 2 is clearly seen. The control scheme block diagram is shown in Fig. 11, with the additional integral compensation required to obtain zero

steady-state error in i'_q. This scheme has been implemented in the ASVC scaled model with a closed-loop control bandwidth set to approximately 200 rad/s. This makes it possible to swing between full inductive mode and full capacitive mode in slightly more than a quarter of a cycle.

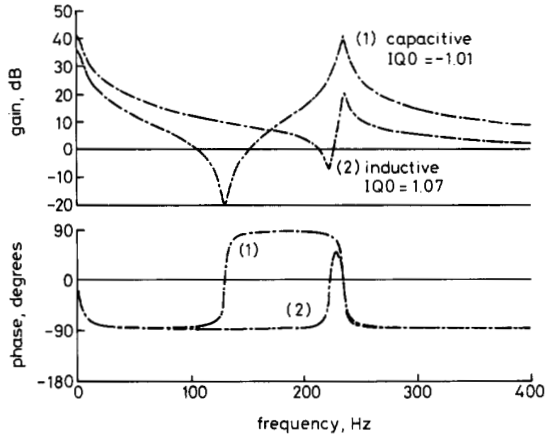

Fig. 10B *Transfer function* $\Delta Q'(s)/\Delta\alpha(s)$

$\frac{\Delta i'_q}{\Delta\alpha} - g(i'_{q0} - i'_{q0x})\frac{\Delta v'_{dc}}{\Delta\alpha}$ $g = 2.0$

3 Line voltage unbalance and harmonic distortion

With balanced sinusoidal line voltage and an inverter pulse number of 24 or greater, and ASVC draws no low-order harmonic currents from the line. However, harmonic currents of low order do occur when the line voltage is unbalanced or distorted. As might be expected from a nonlinear load, the ASVC currents include harmonics not present in the line voltage. It is important to understand ASVC behaviour under these conditions as it can influence equipment rating and component selection.

The ASVC harmonic currents can be calculated by postulating a set of harmonic voltage sources in series with the ASVC tie lines as shown in Fig. 12. If we further neglect losses (i.e. $R'_s = 0$, $R'_p = \infty$) and assume the steady-state condition, $\alpha = 0$ and $\omega = \omega_b$, eqns. 19 are modified as follows:

$$p\begin{bmatrix} i'_d \\ i'_q \\ v'_{dc} \end{bmatrix} = \begin{bmatrix} 0 & \omega_b & \frac{k\omega_b}{L} \\ -\omega_b & 0 & 0 \\ \frac{-3}{2}kC'\omega_b & 0 & 0 \end{bmatrix}\begin{bmatrix} i'_d \\ i'_q \\ v'_{dc} \end{bmatrix} - \frac{\omega_b}{L}\begin{bmatrix} |v'| + v'_{hd} \\ v_{hq} \\ 0 \end{bmatrix} \tag{26}$$

where v'_{hd} and v'_{hq} are the d and q components of the harmonic voltage vector. Eqns. 26 are linear and can be solved using Laplace transforms. Consider the effect of a single balanced harmonic set of order n where negative values of n denote negative sequence. The associated harmonic voltage vector has magnitude, v'_h and rotates with angular velocity $n\omega_b$. In the synchronous reference frame it rotates with angular velocity $(n-1)\omega_b$ as shown in Fig. 13 and

$$v'_{hd} = v'_h \cos[(n-1)\omega_b t]$$
$$v'_{hq} = v'_h \sin[(n-1)\omega_b t] \tag{27}$$

These sinusoidal inputs on the d- and q-axes give rise to sinewave responses i'_{hd}, i'_{hq}, and v'_{hdc} of frequency $(n-1)\omega_b$. Generally i'_{hd} and i'_{hq} do not form a balanced two-phase sinusoidal set. They can be resolved into a positive-sequence set and a negative-sequence set using normal two-phase phasor symmetrical components. We thus find two distinct current component vectors in response to the n-order harmonic voltage vector. Within the synchronous reference frame, these rotate with frequency $(n-1)\omega_b$ and $(1-n)\omega_b$, respectively. The corresponding ASVC line currents have frequencies $n\omega_b$ and $(2-n)\omega_b$, respectively. Note also that the inverter

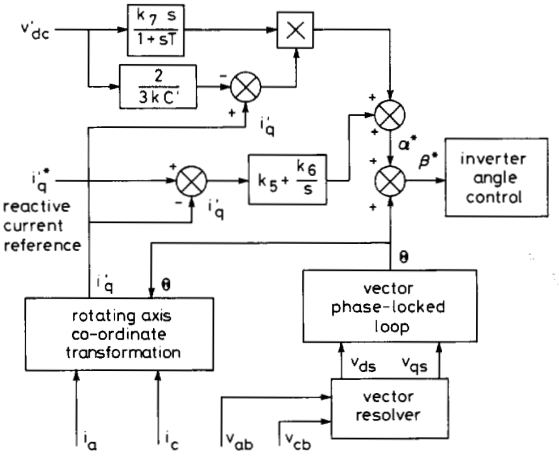

Fig. 11 *Block diagram for inverter Type II control*

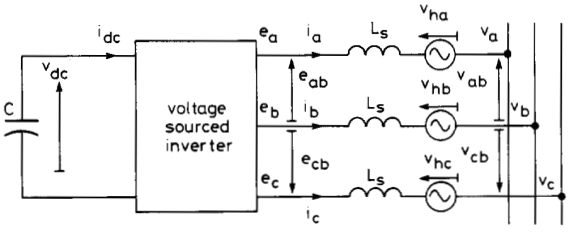

Fig. 12 *ASVC equivalent circuit with harmonic voltage sources*

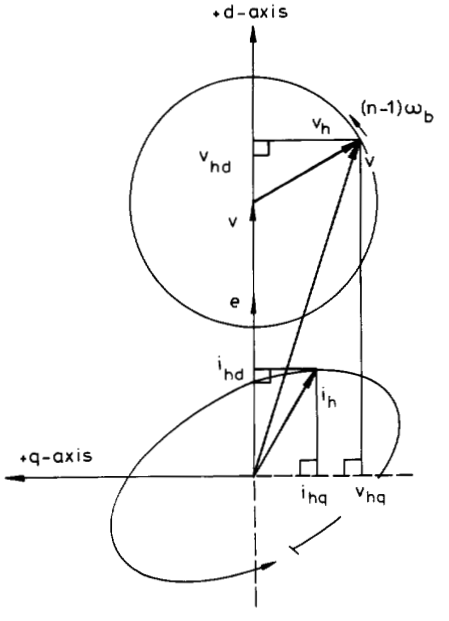

Fig. 13 *Harmonic vectors in the synchronous reference frame*

develops an alternating voltage component of frequency $(n-1)\omega_b$ at its DC terminals.

Eqns. 26 and 27 have been solved to obtain algebraic expressions for the magnitudes of these harmonic currents in the particular case where $n = -1$ (i.e. fundamental negative sequence voltage.) In this case, the ordinals of the harmonic currents are -1 and 3, and the magnitudes are calculated from the following:

$$|i'_{-1}| = \frac{v'_h\left[1-\frac{k^2C'}{8L'}\right]}{L'\left[1-\frac{k^2C'}{2L'}\right]} \tag{28}$$

$$|i'_3| = \frac{v'_h}{4L'\left[1-\frac{2L'}{k^2C'}\right]} \tag{29}$$

These expressions have been evaluated using typical parameters with $v'_h = 1$ p.u., and are plotted against per-unit capacitive reactance in Fig. 14. Notice that for $C' = 2L'/k^2$ both i'_{-1} and i'_3 become infinite. This condition occurs if the second harmonic of the line frequency is equal to the ASVC-resonant-pole frequency defined in eqn. 23. Also, when $C' = 8L'/k^2$, i'_{-1} is zero and the ASVC draws no negative-sequence fundamental current from the line.

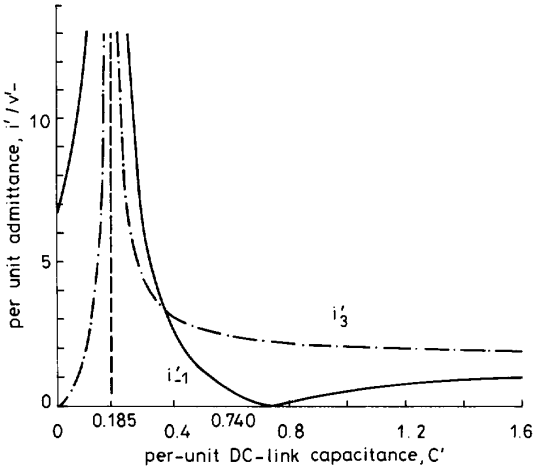

Fig. 14 *ASVC current components with fundamental negative-sequence voltage on the line*
$k = 4/\pi$, $L = 0.15$ p.u., $R_s = 0$, $R_p = \infty$

4 Experimental results from ASVC scaled model

It is beyond the scope of this paper to discuss the EPRI ASVC scaled model in detail. However, two sets of measured waveforms from the model are presented in Figs. 15 and 16 to illustrate the system behaviour under transient conditions. Fig. 15 shows the dynamic response of the instantaneous reactive current controller. In this case a squarewave reference, i'^*_q, is injected, and the oscillogram shows i'_q, α, and the ASVC line currents. Fig. 16 shows the ASVC response to a simulated transient unbalanced fault. In this case, the full ASVC control system is functional and i'^*_q comes from the system voltage controller. Initially, the ASVC is supplying 1 p.u. capacitive VARS to the line. A phase-to-neutral fault, lasting approximately five cycles, is simulated and the oscillogram shows the associated ASVC currents. Note that the reactive current reference, i'^*_q is limited in magnitude to 2 p.u.

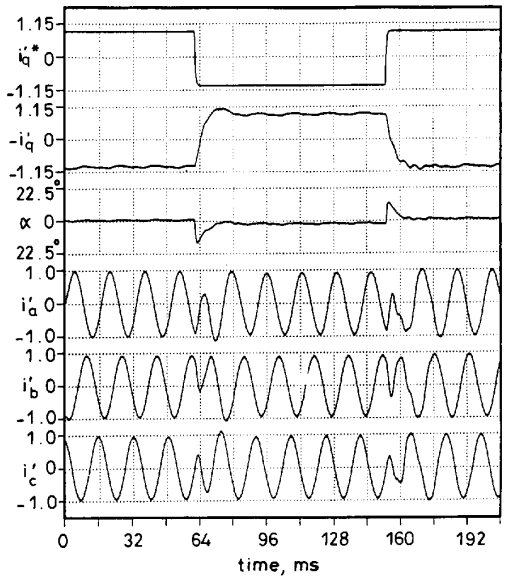

Fig. 15 *Measured transient response of reactive-current control system*

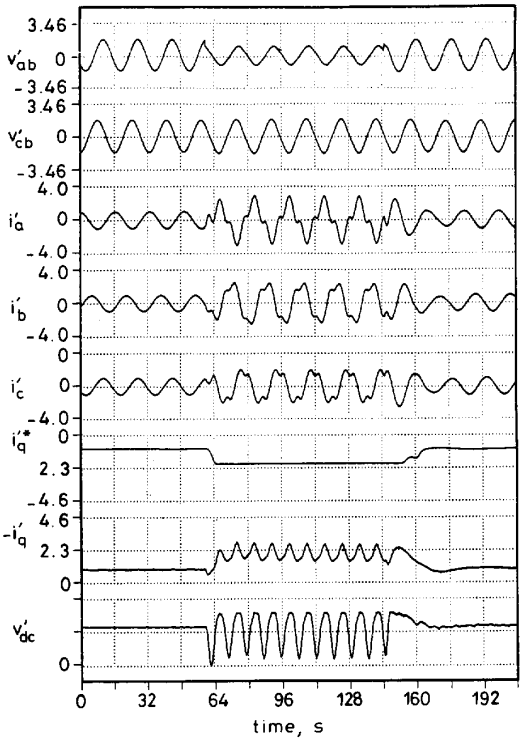

Fig. 16 *ASVC system response to line-to-neutral fault*

5 Conclusions

There is every indication that ASVCs will be an important part of power transmission systems in the future. A sound analytical basis has now been established for studying their dynamic behaviour. The mathematical model derived here can readily be extended to represent

the ASVC in broader system studies. The ASVC analysis has also led to control-system designs for both Type I and Type II voltage-sourced inverters. The Type II inverter control is particularly significant because it makes it possible to obtain excellent dynamic performance from the lowest cost inverter and transformer combination.

6 References

1 GYUGYI, L., *et al.*: 'Advanced static VAR compensator using gate turn-off thyristors for utility applications'. CIGRE, Paper 23–203, 199.

2 EDWARDS, C.W., *et al.* :'Advanced static VAR generator employing GTO thyristors'. IEEE PES Winter Power Meeting, Paper 38WM109-1, 1988

3 HINGORANI, N.G.: 'High power electronics and flexible AC transmission system', *IEEE Power Eng. Rev.*, 1988

4 Electric Power Research Institute: 'Development of an advanced static VAR compensator'. Contract RP3023-1

5 PARK, R.H.: 'Definition of an-ideal synchronous machine and formula for the armature flux linkages', *General Electric Review*, 1928, **31**, pp.

6 LYON, W.V.: 'Transient analysis of alternating current machinery' (John Wiley & Sons, New York, 1954)